DOI: 10.1002/ejic.200901198

# The Nature of the Phosphazene Nitrogen–Metal Bond: DFT Calculations on 2-(Pyridyloxy)cyclophosphazene Complexes

**Ross J. Davidson,[a] Eric W. Ainscough,*[a] Andrew M. Brodie,*[a] John A. Harrison,[b] and Mark R. Waterland[a]**

**Keywords:** Phosphazenes / Transition metals / Density functional calculations / Metal–ligand bonds

The metal–nitrogen bond in six-coordinate complexes $[ML^1Cl]^+$ (M = Co, Ni, Cu or Zn) of (pyridyloxy)cyclophosphazene, five-coordinate complexes $[ML^1Cl_2]$ (M = Cu or Zn) of green-$[NiL^1Cl_2]$, and dimetallic complexes $[L^2(CuCl_2)_2]$, $[L^3(CuCl)_2]^{2+}$ and $[L^3(CuCl_2)_2]$ [$L^1$ = hexakis(2-pyridyloxy)-cyclotriphosphazene, $L^2$ = hexakis(4-methyl-2-pyridyloxy)-cyclotriphosphazene or $L^3$ = octakis(4-methyl-2-pyridyloxy)-cyclotetraphosphazene] of red-$[NiL^1Cl_2]$, has been investigated by using density functional theory (DFT) and natural bond order (NBO) analysis. The calculations show that the divalent metal ions bind to the phosphazene ring nitrogen by a σ-type bond and that the lengthening of the PN bonds, which flank the metal coordination site, can be explained as a result of electron density that is transferred from PN bonding orbitals to the 4s orbital of the metal ion rather than a decrease in the π component of the bond as suggested by earlier models. It can be assumed that this explanation of the bonding is valid for the wide range of metallo-phosphazene complexes and that metal ions will bind to the PN backbone of polyphosphazenes in a similar manner.

## Introduction

Cyclophosphazene scaffolds, with their $[–NPX_2–]_n$ repeating unit, continue to provide a rich variety of multimodal ligand systems. The skeletal ring nitrogen atoms themselves can bind to transition metals, especially if their basicity is enhanced by the attachment of electron-releasing substituents, e.g. X = dimethylamino, to the skeletal phosphorus atoms. An alternative approach, which has yielded a much greater array of complexes in which the skeletal nitrogen is coordinated, is to attach appropriate pendant donor groups to the skeletal ring phosphorus atoms, e.g. X = 3,5-dimethylpyrazolyl[1] or 2-pyridyloxy.[2] Such ligands are designed to simultaneously chelate to transition metal ions via both the skeletal ring nitrogen and the pendant donor atom. More recently, polymeric metallo-phosphazene materials have been investigated because of their potential uses such as electroconductive and electroresponsive polymers, catalytic substrates, nonlinear optics materials and anticancer agents.[3] Although most of the metallo-polyphosphazenes characterized to date involve metal ion binding exclusively to pendant donors without involvement of the backbone skeletal nitrogen atoms of the polymer chain, there is evidence that $PtCl_2$ units are doing so in poly[bis(methylamino)phosphazene.[4] and NMR spectroscopic and molecular dynamic studies indicate that significant lithium ion interaction with the backbone nitrogen occurs in polyphosphazene solid polymer electrolytes.[5]

Small-molecule cyclophosphazenes play a crucial role in the development and understanding of new polyphosphazene polymeric materials including the nature of the multiple bonding along the PN backbone. A number of attempts have been made to explain the multiple character of the PN bond with models evolving from those proposed by Craig and Paddock[6] and Dewar[7] which use the 3d and 2p orbitals on the phosphorus and nitrogen atoms respectively to form π-bonds to one that is predominantly ionic with a negative hyperconjugation component being required for a complete description (henceforth called the Chaplin model[8]). Calculations show that phosphorus 3d orbitals do not play a significant role in phosphazene–nitrogen bonding.

As observed over 30 years ago by Paddock,[9] when a cyclophosphazene ring nitrogen is protonated or coordinated to a metal ion, the flanking PN bond lengths were always longer than the other ring PN bonds or the PN bonds in the uncoordinated ligand (Figure 1). In addition, the lengthening appeared to be independent of the substituents on the phosphorus atoms. Paddock assumed that the PN bond lengthening was a result of the nitrogen 2p orbital becoming orientated to permit bonding to the metal, thereby preventing π bonding with the phosphorus 3d orbital. Although the Paddock and Dewar models have been superseded by ab initio investigations such as those of

[a] Chemistry – Institute of Fundamental Sciences, Massey University,
Private Bag 11 222, Palmerston North, New Zealand
Fax: +64-6-3505682
E-mail: e.ainscough@massey.ac.nz
a.brodie@massey.ac.nz
[b] Chemistry – Institute of Natural Sciences, Massey University, Private Bag 102 904, Auckland, New Zealand
Supporting information for this article is available on the WWW under http://dx.doi.org/10.1002/ejic.200901198.

  

Chaplin et al. for uncoordinated cyclophosphazenes, there has not been an attempt to determine the nature of the phosphazene-nitrogen metal bonding using the most recent bonding model or to explain the lengthening of the flanking PN bonds on metal coordination. Hence in this study we report the results of an investigation using Density Functional Theory (DFT) calculations to probe the interaction between a cyclophosphazene and a divalent transition-metal ion using the three related ligands – hexakis(2-pyridyloxy)cyclotriphosphazene ($L^1$),[10] hexakis(4-methyl-2-pyridyloxy)cyclotriphosphazene ($L^2$),[2h] and octakis(4-methyl-2-pyridyloxy)cyclotetraphosphazene ($L^3$)[11] (see Figure 2). These ligands were chosen as they are able to coordinate to a variety of first row transition metals with a range of known geometries.[2] Moreover, the presence of the flexible phenoxy hinge linking the pyridyloxy pendant arms to the phosphazene ring allows the formation of six-membered chelate rings without significantly distorting the planarity of the $P_3N_3$ ring.

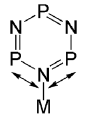

Figure 1. Behaviour of the phosphazene when a metal ion coordinates: (i) the metal coordinates to the ring nitrogen, (ii) the flanking PN bonds lengthen, (iii) the lengthening is independent of the substituent on the phosphorus atoms.

Two publications have previously explored the interaction of transition-metal ions with cyclophosphazenes. Recently we reported DFT calculations on the dimetallic complexes, $[L^2(CuCl_2)_2]$ and $[L^3(CuCl)_2]^{2+}$, and identified "electron-density-bridge" molecular orbitals which involved Cu 3d orbitals overlapping with the non-bonding, N-based molecular orbitals on the phosphazene rings as the pathway for the weak antiferromagnetic coupling observed between the copper(II) centres.[2c] Gall and Breza[12] carried out QTAIM (quantum theory of atoms-in-molecule) topological electron density analyses of complexes of $L^1$ with $Ni^{II}$ and $Zn^{II}$ and concluded that the metal–nitrogen bonds in the phosphazene ring were stronger and more polar than the bonds to the pendant pyridine nitrogen donors. In addition they noted that for the red-$[NiL^1Cl_2]$ five-coordinate complex the values for the bond ellipticities[12] are significantly different from zero at the M–N and M–Cl bond critical points, indicative of π contributions to these bonds.

## Computational Methodology

All of the optimizations and frequency calculations were carried out using the Gaussian03[13] and GaussView[14] suite of programs. The DFT calculations were carried out at the B3LYP level with a 6-31G(d) basis set. In order to determine the validity of the DFT models, a comparison was made between the bond lengths from the X-ray structures of known or closely related complexes[2c,2e,2h] and the calcu-

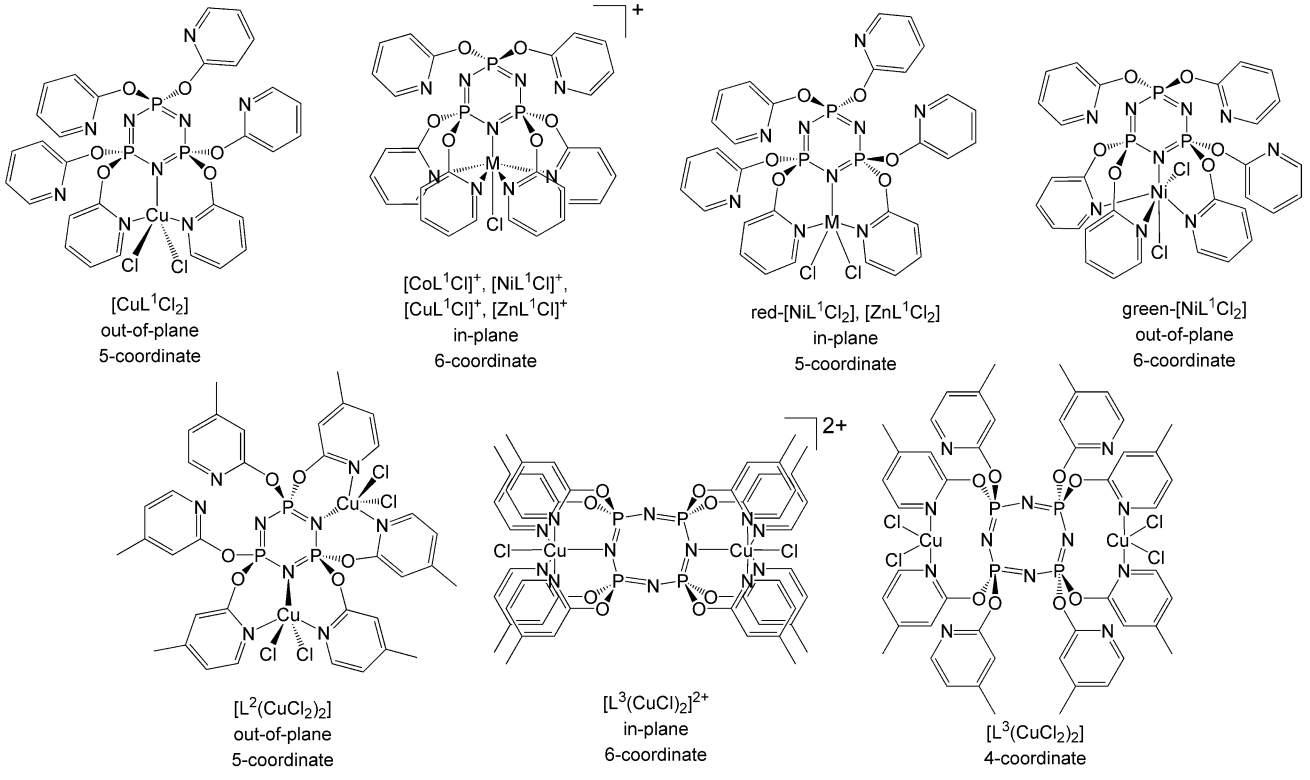


Figure 2. The pyridyloxy-substituted cyclophosphazene transition metal complexes used in the DFT calculations. In-plane and out-of-plane refers to the position of the metal ion relative to the plane of the phosphazene ring.

  

lated bond lengths. The results displayed the typical overestimation associated with DFT calculations[15] although the differences were less than 2% for all bonds (see Table S1, Supporting Information). A comparison was also made between the measured and calculated infrared spectra. Although very similar, there were differences between the simulated and measured spectra, most likely due to solid state effects (see Table S2, Supporting Information). The spin multiplicities for the complexes were confirmed by measuring the magnetic susceptibilities and the comparison of simulated UV/Vis spectra (see Table S3, Supporting Information).

To examine the effect of coordination of the phosphazene ring nitrogen on the metal 3d orbitals, calculations were also carried out on complexes in which the cyclophosphazene ligand was replaced by one which had 2-hydroxypyridine held in the same orientation about the metal ion as the phosphazene-pyridyloxy pendant arms (see Figure 3 below).

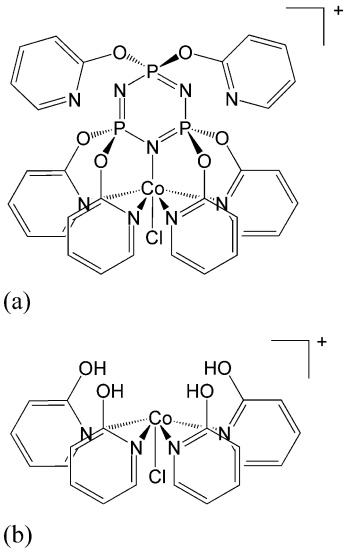


Figure 3. (a) $[CoL^1Cl]^+$ – the parent complex with the complete phosphazene bound to the metal ion. (b) $[Co(HOPy)_4Cl]^+$ – the complex without the phosphazene bound.

## Results and Discussion

### The Classification of the Phosphazene Nitrogen Metal Bond

The first question to answer is does the phosphazene ring nitrogen bind to the metal via a simple σ-type bond or does the bond contain a π-component? A qualitative molecular orbital model for octahedral complexes of the first row transition metals, indicates that for simple σ-donor ligands, the energy of the "$e_g$" ($3d_{x^2-y^2}$ and $3d_{z^2}$) orbitals will be significantly altered, but for π-donors or acceptors, it is the energy of the "$t_{2g}$" ($3d_{xy}$, $3d_{xz}$ and $3d_{yz}$) orbitals that will change.[16] To identify which 3d orbitals are most affected by phosphazene binding, partial molecular orbital diagrams for the complexes based on 3d orbitals were generated and compared with those which did not have the phosphazene attached (see Figure 3).

Figure 4 shows a MO diagram for the octahedral, in-plane complex, $[CoL^1Cl]^+$. All complexes with this geometry have the metal ion coordinated to the phosphazene ring nitrogen, a chloride ligand and four pendant pyridine donors in an approximately $C_{4v}$ geometry. Only the $\beta$ orbitals are depicted because, unless the complex is a diamagnetic singlet, these show a greater change in energy than the $\alpha$ orbitals. Figure 4 shows that the $\beta 3d_{z^2}$ orbital of the metal ion is significantly lowered in energy when coordinated to the phosphazene ring nitrogen. A similar effect is also seen for the analogous nickel(II) and copper(II) complexes, $[NiL^1Cl]^+$ and $[CuL^1Cl]^+$ (see Figure 5) but not for the diamagnetic zinc(II) complex, $[ZnL^1Cl]^+$. For this latter complex, there is little change in the order of the d orbital energies. Zinc has a full 3d electron shell and is, therefore, unable to accommodate extra electron density to the same extent as the other metal ions. It is noted that the shift in energy is greatest for the cobalt(II) and nickel(II) complexes (–0.10646 eV and –0.10928 eV, respectively) than for the copper(II) complex (–0.01551 eV). This difference is the result of the metals with the lower occupancy in the 3d shell (i.e. cobalt and nickel) being able to access greater electron density from the phosphazene ring nitrogen, hence resulting in a greater perturbation of their d orbital energies. The relative lowering in energy of the $\beta 3d_{z^2}$ orbitals is confirmed by comparing the occupancy of these orbitals of the complexes (Figure 6).

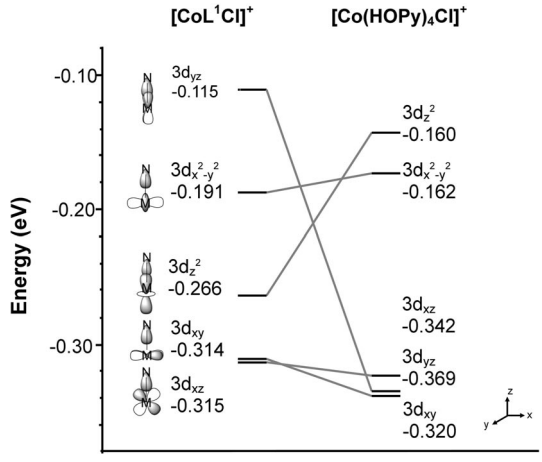


Figure 4. Partial MO energy level diagrams for $[CoL^1Cl]^+$ and $[Co(HOPy)_4Cl]^+$ comparing the metal ion $\beta 3d$ orbitals with, and without, the phosphazene bound.

Figure 6 shows that there is an increase in the $\beta 3d_{z^2}$ orbital occupancy once the metal binds to the phosphazene ring nitrogen. This also confirms that the change in electron density at the metal centre is inversely proportional to the occupancy of the 3d shell, i.e. $[CoL^1Cl]^+$ has an occupancy increase of 0.6479 $e^-$, but for $[CuL^1Cl]^+$ the difference is 0.0064 $e^-$. Representations of the molecular orbitals responsible for this bonding are shown below (see Figure 7).

  

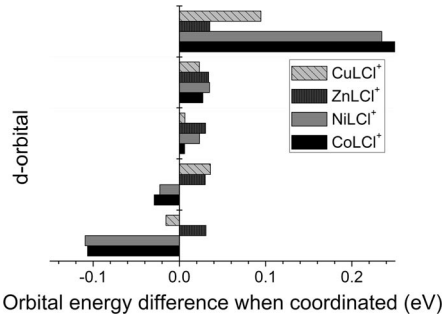


Figure 5. Comparison of the effect the phosphazene ring nitrogen has on the energy of the on the $\beta 3d_{z^2}$ orbitals when binding to the metal ion in the octahedral, in-plane, six-coordinate, $[ML^1Cl]^+$ (M = Cu, Zn, Ni and Co) complexes.

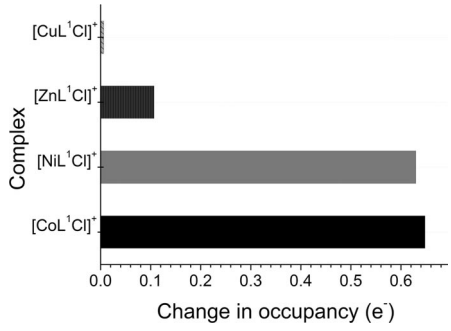


Figure 6. Difference in the occupancy of the $\beta 3d_{z^2}$ orbitals with, and without, the phosphazene ring nitrogen bound to the metal for the $[ML^1Cl]^+$ (M = Cu, Zn, Ni and Co) complexes.

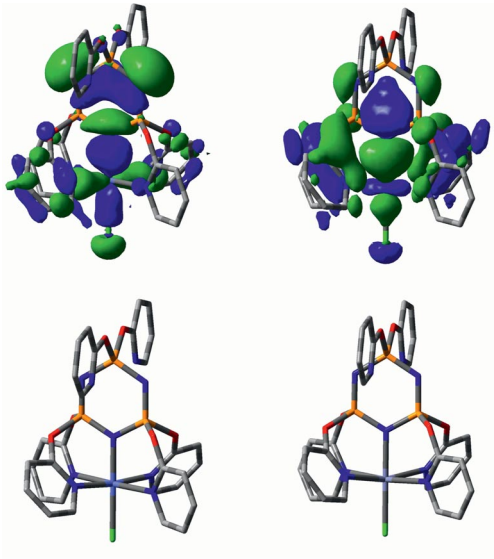


Figure 7. (a) Metal bonding orbital for $[ML^1Cl]^+$ (M = Co, Ni and Cu). (b) Metal bonding orbital for $[ZnL^1Cl]^+$.

In both cases, the phosphazene ring nitrogen–metal interaction can be classified as a σ-bond. The metal-based component for the cobalt, nickel and copper complexes is mainly of $3d_{z^2}$ character, with small a contribution from the $3d_{x^2-y^2}$ orbital (see Table S4.1). The involvement of the "$e_g$"-type orbitals in bonding, rather than the "$t_{2g}$" orbitals, is typical of σ donors as is its stabilization.[16]

To confirm that this was not simply the result of the geometry of the complexes, both the in-plane five-coordinate and the out-of-plane 5- and six-coordinate species (Figure 1) were investigated. It was found that the in-plane five-coordinate species, red-$[NiL^1Cl_2]$ and $[ZnL^1Cl_2]$, also showed a stabilization of an "$e_g$"-type orbital. In this case it was the $3d_{x^2-y^2}$ metal orbital rather than the $3d_{z^2}$ because the latter is involved in an axial bond with the pyridine donors (see Table S4.1). The significant contributions of both the N $2p_x$ and $2p_z$ orbitals seen in the red-$[NiL^1Cl_2]$ M–L bonding orbital is indicative of an additional π contribution for the bond and is consistent with the non-zero bond ellipticity calculated by Gall and Breza.[12]

The out-of-plane species, five-coordinate complex, $[CuL^1Cl_2]$ and six-coordinate green-$[NiL^1Cl_2]$ were quite different in geometry. The single-crystal X-ray structure of the nickel complex[2e] shows the metal centre is only 12° out from the plane of the phosphazene ring; hence it behaves similarly to the other six-coordinate species by bonding predominately via the $3d_{z^2}$ metal orbital. In contrast, for five-coordinate $[CuL^1Cl_2]$, the metal ion was 25° out of the phosphazene ring plane.[2h] As for the other five-coordinate complexes, the $3d_{x^2-y^2}$ metal orbital makes a significant contribution to the phosphazene nitrogen–metal bond but because the metal is far enough out of plane, the $3d_{yz}$ orbital also contributes (see Table S4.2).

Finally, calculations on the dimetallic complexes, $[L^2(CuCl_2)_2]$ and $[L^3(CuCl)_2]^{2+}$, showed that "$e_g$"-type orbitals were involved in bonding to the phosphazene ring nitrogen for both species. However, in the former complex, as for the five-coordinate $[L^1(CuCl_2)_2]$, the "$t_{2g}$" orbitals also make a contribution.

Natural bond orbital (NBO) $E_2$ values[17] were used to determine the origin of the electron density donated to the metal ion. The $E_2$ values are a measure of the interaction strength between a donor NBO and an acceptor NBO, as defined by Equation (1).

$$E_2 = \frac{q_i[F(i,j)]^2}{f_i - f_j} \quad (1)$$

$F(i,j)$ are the off-diagonal Fock matrix elements, $f_i - f_j$ are the energy differences between the NBOs, which are then weighted by $q_i$, the occupancy of the donor NBO. Figure 8 shows a comparison of the only significant interaction between the metal and phosphazene ring nitrogen using $E_2$ interaction energies.

The $E_2$ energies indicate the metal ions in the in-plane, six-coordinate complexes, $[ML^1Cl]^+$ (M = Co, Ni, Cu and Zn) interact more strongly with the phosphazene ring nitrogen than those in the in-plane, five-coordinate red-$[NiL^1Cl_2]$ and $[ZnL^1Cl_2]$. The out-of-plane species, $[CuL^1Cl_2]$, and the other the six-coordinate green-$[NiL^1Cl_2]$, have even weaker interactions. Dimetallic

  

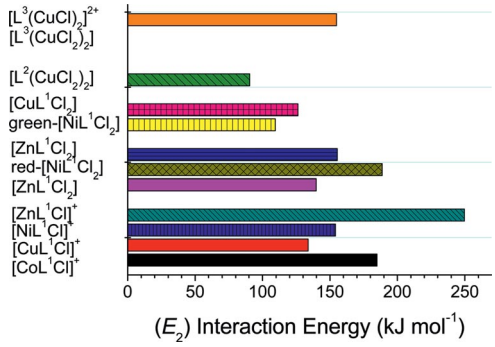


Figure 8. Phosphazene ring nitrogen–metal bond energies $E_2$.

$[L^2(CuCl_2)_2]$ shows much weaker metal–nitrogen bonding than its single metal ion analogue $[CuL^1Cl_2]$, probably as a result of the reduction of electron density in the phosphazene ring arising from two $Cu^{II}$ ions binding. Similarly dimetallic $[L^3(CuCl)_2]^{2+}$ shows the same trend relative to its single copper species, $[CuL^1Cl_2]$. As expected[2c] the dimetallic complex, $[L^3(CuCl_2)_2]$, does not show any bonding to the phosphazene ring nitrogen (see Figure 9).

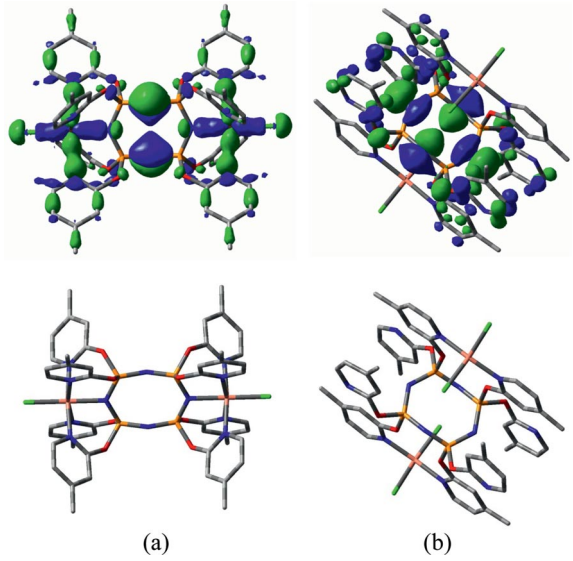


Figure 9. (a) The metal bonding orbital for $[L^3(CuCl)_2]^{2+}$. (b) The non-metal bonding orbital for $[L^3(CuCl_2)_2]$.

The $E_2$ calculations show the phosphazene orbitals that donate to the metal ions are essentially a lone pair from the phosphazene ring nitrogen which consists of 33% s and 66% p character for a $P_3N_3$ ring, and 23% s and 77% p character for a $P_4N_4$ ring. Using Pauling's valence bond terminology, these could be crudely called $sp^2$ orbitals (see Figure 10). The $P_4N_4$ donor orbital is not perfectly $sp^2$ because when the $Cu^{II}$ ion coordinates the PNP bond opens up to 128°, from about 120° seen for $P_3N_3$ rings.

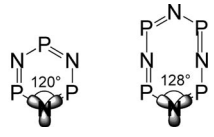


Figure 10. Schematic view of the phosphazene ring nitrogen bonding orbital (a) $P_3N_3$ ring. (b) $P_4N_4$ ring.

## The Lengthening of the PN Bonds Flanking the Coordination Site

The DFT calculations discussed above indicate that when a metal ion binds to a cyclophosphazene via a ring nitrogen it acts as $\sigma$-donor. However, this description does not explain why the PN bonds flanking the coordination site typically lengthen when a transition metal is coordinated as seen for example in $[CuL^1Cl]^+$ [flanking PN bond lengths 1.591(2)–1.601(3) Å, other PN bond lengths 1.550(3)–1.589(3) Å][2h] and other complexes.[1b] An analysis of the $E_2$ values shows that for all the complexes there is an interaction of approximately 5–20 kJ mol$^{-1}$ resulting from the flanking PN bonds donating electron density into the 4s orbitals of the coordinated metal ions (see Figure 11), rather than the PN antibonding orbitals accepting electron density from metal ion orbitals.

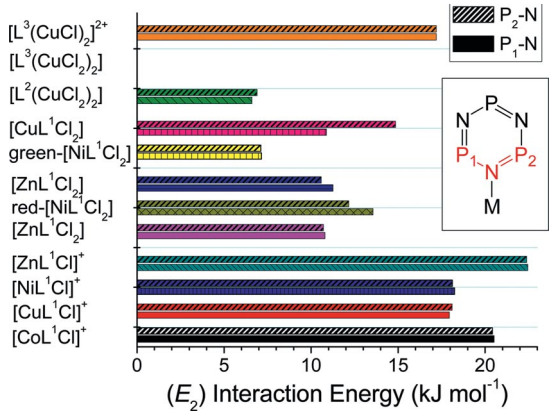


Figure 11. Comparison of the $E_2$ flanking PN bond interactions with the 4s orbital of the metal ion for the complexes.

The dimetallic species have similar $E_2$ interaction strengths as their single metal analogues, e.g. $[L^3(CuCl)_2]^{2+}$ cf. $[CuL^1Cl]^+$, which suggests that the interaction is localized and depends on the ability of the metal ion to accept the electron density. The observations that the $E_2$ interaction strength is greater in the six-coordinate in-plane species than in the five-coordinate in-plane species is consistent with a dependence on the distance between the flanking PN bonds and the metal ion, e.g. for $[CuL^1Cl]^+$ the Cu–N distance is 1.993(3) Å[2e] and for $[CuL^1Cl_2]$ it is 2.264(2) Å.[2h] To confirm this, the relationship of the $E_2$ interaction strength with the calculated metal ion distance was calculated.

Figure 12 shows that there is a linear relationship between the donor-acceptor $E_2$ interaction energy and the metal–ring nitrogen distances as expected for a significant involvement of the 4s orbital. The comparison between the

  

six-coordinate, in-plane and five-coordinate, out-of-plane species is independent of the coordination geometry around the metal ion.

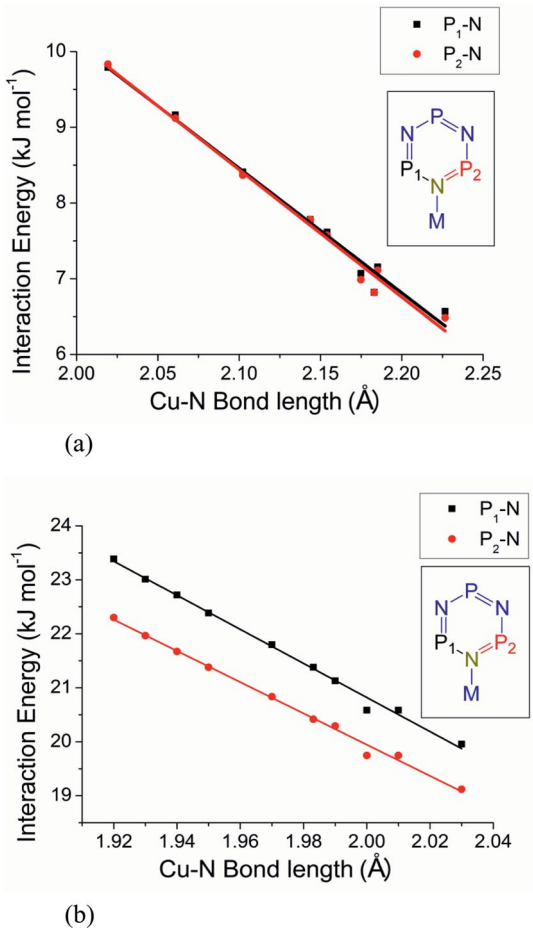


Figure 12. The calculated $E_2$ interaction energy vs. the metal–nitrogen distance. (a) $[CuL^1Cl_2]$ (b) $[CuL^1Cl]^+$.

Comparison of the flanking PN bond occupancy vs. the interaction energy (Figure 13) reveals a linear relationship for the nickel, copper and cobalt complexes $[ML^1Cl]^+$. Showing that, for these complexes, the PN bond occupancy is directly proportional to the donor-acceptor interaction energy. Therefore, the interaction between the metal 4s orbital and phosphazene ring affects the bonding in the ring itself, and in particular, in the flanking PN bonds.

The zinc complex $[ZnL^1Cl]^+$, however, is an outlier, which may be due to its full 3d orbital resulting in a higher occupancy of the 4s orbital and hence lower transfer of electron density from the flanking PN bond. A direct relationship between the bond lengthening and $E_2$ interaction strength was not found, possibly due to substituent effects.

Comparison between the PN bond donor and the bonding contributions for the Chaplin model[8,12] shows that the electron density originates from the ionic bonding contribution (see Table S6). It is primarily the reduction of this bonding contributor that causes the lengthening of the flanking PN bonds (Figure 14).

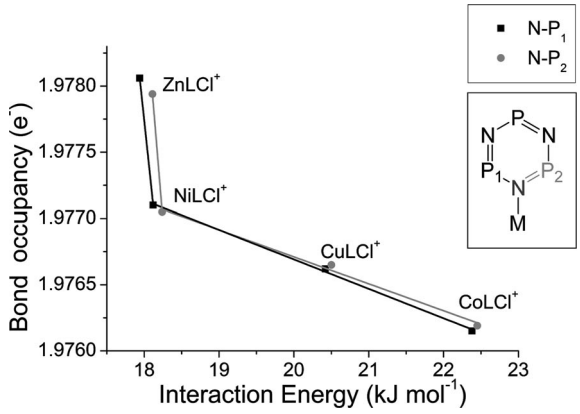


Figure 13. $E_2$ Interaction energy vs. flanking PN bond occupancy.

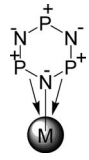

Figure 14. Schematic view of the ionic PN bonding donating electron density to the 4s orbital of the metal ion.

## Conclusions

DFT calculations carried out on complexes of the divalent metal ions, Co, Ni, Cu and Zn, with pyridyloxy-substituted cyclotri- and cyclotetraphosphazene ligands $L^1$, $L^2$ and $L^3$, show that the phosphazene ring nitrogen acts as a σ donor. The lengthening of the PN bonds flanking the metal coordination site can be explained as a result of electron density that is transferred from PN bonding orbitals to the 4s orbital of the metal ion and not a decrease in the extent of π-bonding as suggested by earlier models. The ionic component of the PN bond is reduced upon metal coordination, which is consistent with the Chaplin phosphazene bonding model.[8] This model may be applied to the wide range of metallo-phosphazene complexes and also to the binding of metals in the backbone of polyphosphazenes.

**Supporting Information** (see also the footnote on the first page of this article): Material for the DFT calculations.

## Acknowledgments

We are grateful for financial support from the RSNZ Marsden Fund (MAU208). We also thank Professor P. A. Schwerdtfeger and the Theochem group for access to the Double Helix parallel-computing facility (Massey University Albany) and Dr. A. B. Chaplin for assistance with NBO calculations.

[1] a) V. Chandrasekhar, P. Thilagar, B. Murugesa Pandian, *Coord. Chem. Rev.* **2007**, *251*, 1045–1074; b) V. Chandrasekhar, S. Nagendran, *Chem. Soc. Rev.* **2001**, *30*, 193–203.

[2] a) V. Chandrasekhar, B. Murugesa Pandian, R. Azhakar, *Polyhedron* **2007**, *27*, 255–262; b) V. Chandrasekhar, B. M. Pandian, R. Azhakar, *Inorg. Chem.* **2006**, *45*, 3510–3518; c) E. W. Ainscough, A. M. Brodie, R. J. Davidson, B. Moubaraki, K. S.

  

Murray, C. A. Otter, M. R. Waterland, *Inorg. Chem.* **2008**, *47*, 9182–9192; d) E. W. Ainscough, A. M. Brodie, A. Derwahl, S. Kirk, C. A. Otter, *Inorg. Chem.* **2007**, *46*, 9841–9852; e) E. W. Ainscough, A. M. Brodie, C. V. Depree, C. A. Otter, *Polyhedron* **2006**, *25*, 2341–2352; f) E. W. Ainscough, A. M. Brodie, C. V. Depree, G. B. Jameson, C. A. Otter, *Inorg. Chem.* **2005**, *44*, 7325–7327; g) E. W. Ainscough, A. M. Brodie, C. V. Depree, *J. Chem. Soc., Dalton Trans.* **1999**, 4123–4124; h) E. W. Ainscough, A. M. Brodie, C. V. Depree, B. Moubaraki, K. S. Murray, C. A. Otter, *Dalton Trans.* **2005**, 3337–3343.

[3] P. Pertici, G. Vitulli, M. Gleria, G. Facchin, R. Milani, R. Bertani, *Macromol. Symp.* **2006**, *235*, 98–114.

[4] R. W. Allen, J. P. O'Brien, H. R. Allcock, *J. Am. Chem. Soc.* **1977**, *99*, 3987–3991.

[5] a) Y. Wang, P. B. Balbuena, *J. Phys. Chem. B* **2004**, *108*, 15694–15702; b) T. A. Luther, F. F. Stewart, J. L. Budzien, R. A. LaViolette, W. F. Bauer, M. K. Harrup, C. W. Allen, A. Elayan, *J. Phys. Chem. B* **2003**, *107*, 3168–3176.

[6] D. P. Craig, N. L. Paddock, *Nature* **1958**, *181*, 1052–1053.

[7] M. J. S. Dewar, E. A. C. Lucken, M. A. Whitehead, *J. Chem. Soc.* **1960**, 2423–2429.

[8] A. B. Chaplin, J. A. Harrison, P. J. Dyson, *Inorg. Chem.* **2005**, *44*, 8407–8417.

[9] a) H. P. Calhoun, N. L. Paddock, J. N. Wingfield, *Can. J. Chem.* **1975**, *53*, 1765–1774; b) H. P. Calhoun, R. T. Oakley, N. L. Paddock, J. Trotter, *Can. J. Chem.* **1975**, *53*, 2413–2418.

[10] G. A. Carriedo, P. Gomez Elipe, F. J. Garcia Alonso, L. Fernandez-Catuxo, M. R. Diaz, S. Garcia Granda, *J. Organomet. Chem.* **1995**, *498*, 207–212.

[11] E. W. Ainscough, A. M. Brodie, A. Derwahl, *Polyhedron* **2003**, *22*, 189–197.

[12] M. Gall, M. Breza, *Polyhedron* **2009**, *28*, 521–524.

[13] M. J. Frisch, G. W. Trucks, H. B. Schlegel, G. E. Scuseri, M. A. Robb, J. R. Cheeseman, J. J. A. Montgomery, T. Vreven, K. N. Kudin, J. C. Burant, J. M. Millam, S. S. Iyengar, J. Tomasi, V. Barone, B. Mennucci, M. Cossi, G. Scalmani, N. Rega, G. A. Petersson, H. Nakatsuji, M. Hada, M. Ehara, K. Toyota, R. Fukuda, J. Hasegawa, M. Ishida, T. Nakajima, Y. Honda, O. Kitao, H. Nakai, M. Klene, X. Li, J. E. Knox, H. P. Hratchian, J. B. Cross, C. Adamo, J. Jaramillo, R. Gomperts, R. E. Stratmann, O. Yazyev, A. J. Austin, R. Cammi, C. Pomelli, J. W. Ochterski, P. Y. Ayala, K. Morokuma, G. A. Voth, P. Salvador, J. J. Dannenberg, V. G. Zakrzewski, S. Dapprich, A. D. Daniels, M. C. Strain, O. Farkas, D. K. Malick, A. D. Rabuck, K. Raghavachari, J. B. Foresman, J. V. Orti, Q. Cui, A. G. Baboul, S. Clifford, J. Cioslowski, B. B. Stefanov, G. Liu, A. Liashenko, P. Piskorz, I. Komaromi, R. L. Martin, D. J. Fox, T. Keith, M. A. Al-Laham, C. Y. Peng, A. Nanayakkara, M. Challacombe, P. M. W. Gill, B. Johnson, W. Chen, M. W. Wong, C. Gonzalez, J. A. Pople, *Gaussian 03*, Revision C.02, Gaussian Inc., Wallingford, **2004**.

[14] R. Dennington II, T. Keith, J. M. Millam, K. Eppinnett, W. L. Hovell, R. Gilliland, *GaussView*, 3.09, Semichem Inc., Shawnee Mission, **2003**.

[15] P. v. R. Schleyer, *Encyclopedia of Computational Chemistry*, New York, J. Wiley, Chichester, **1998**.

[16] D. F. Shriver, P. W. Atkins, *Inorganic Chemistry*, 3rd ed., Oxford University Press, New York, **1999**.

[17] a) F. Weinhold, C. R. Landis, *Chem. Educ.* **2001**, *2*, 91–104; b) J. P. Foster, F. Weinhold, *J. Am. Chem. Soc.* **1980**, *102*, 7211–7218.

Received: December 11, 2009
Published Online: February 25, 2010

  